26th IMEKO TC4 International Symposium
24th International Workshop on ADC and DAC Modelling and Testing
IMEKO TC-4 2023
Pordenone, Italy / September 20-21, 2023

Novel quality assessment protocol based on Kiviat diagram for pulsed wave Doppler diagnostic systems: first results

Giorgia Fiori[1], Gabriele Bocchetta[1], Maurizio Schmid[1], Silvia Conforto[1], Salvatore Andrea Sciuto[1], Andrea Scorza[1]

[1] *Dep. of Industrial, Electronic and Mechanical Engineering, Roma TRE University, Rome, Italy*

***Abstract* – Ultrasound (US) systems are routinely and extensively used in several medical fields despite the lack of an internationally accepted quality standard for their testing. One crucial aspect for Quality Assessment (QA) protocols is the need to summarize the contribution of the large number of existing test parameters in a few meaningful quantities. The study herein proposed fits into this context, focusing on the use of the Kiviat diagram applied to Pulsed Wave Doppler (PWD) equipment QA. Four test parameters, derived from the literature, were objectively assessed through custom-written image analysis-based methods and then scaled for an effective combination. The experimental setup used to collect PWD spectrograms included an intermediate technology level US diagnostic system equipped with a linear array probe and a commercial Doppler flow phantom. Tests were repeated at two Doppler frequencies.**

I. INTRODUCTION

In diagnostic ultrasound (US), Quality Assessment (QA) protocols are deemed necessary in order to monitor the performance level of the imaging equipment over time and detect any non-conformities [1-3]. Progressive worsening of US system performance usually occurs as a slow worsening of the image quality that could impact clinical decision, increasing the risk of misdiagnosis [4-7]. In this regard, many studies in the scientific literature have analysed this process: average annual failure rates of 10% and 14% have been detected for system components and probes, respectively, over a four-year experience [8], and a 40% incidence of defective probes has been found in routine clinical practice [7]. Although several professional organizations attempted to define guidelines for ultrasound QA over the years [9-12], a shared worldwide reference standard has yet to be developed [1,13]. This is associated, among other factors, with the presence of diverse performance parameters, and with the lack of a comprehensive approach to QA [1,3,13]. On this point, Kiviat diagrams have been introduced in [3] to effectively combine experimental test parameters for Color Doppler QA. By calculating the diagram area, it is possible to provide a comprehensive indicator of Color Doppler system performance.

From these considerations, the present study aims at providing the first results of the application of the integrated method proposed in [3] to quantify the overall performance of Pulsed Wave Doppler (PWD) diagnostic systems. Tests were carried out on an intermediate technology level ultrasound system equipped with a linear array probe operating at two Doppler frequencies. PWD performance was assessed in terms of Average Maximum Velocity Sensitivity (AMVS) [14], Velocity Measurements Accuracy (VeMeA), Velocity Profile Discrepancy Index (VPDI) [15,16] and Lowest Detectable Signal (LDS) [17]. Each parameter was estimated from PWD data post-processed through objective image analysis-based methods implemented in MATLAB environment.

II. MATERIALS AND METHODS

A. Experimental setup

The experimental setup consisted of a linear array probe mounted on an intermediate technology level US diagnostic system and a reference test device. The ultrasound probe worked at two operating Doppler

Table 1. Main ultrasound system settings.

Parameter	Setting
B-mode frequency (MHz)	9.0
Doppler frequency (MHz)	$f_1 = 5.0$; $f_2 = 6.3$
Field of view (mm)	70
Wall filter	Minimum
Sample volume length (mm)	1 (AMVS, VeMeA and VPDI) ; 2 (LDS)
Sample volume depth (mm)	40 (AMVS, VeMeA) ; from 35 to 41 (VPDI) ; from 38 to 48 (LDS)
Insonation angle (°)	50
Spectrogram duration (s)	8

frequencies (i.e., the lowest and the central one) by minimizing both pre- and post-processing settings as reported in Table 1.

A commercial flow phantom (Sun Nuclear, Doppler 403TM flow phantom [18]) was included in the setup as reference test device. It consists of a horizontal and a diagonal tube segment (5.0 ± 0.2 mm inner diameter) embedded in a tissue-mimicking material (TMM). A blood-mimicking fluid (BMF) simulating the blood flow is pumped into the circuit in constant or pulsatile mode through an electric flow controller.

PWD spectrograms were collected on a portion of the diagonal segment, by maintaining the ultrasound transducer still in a dedicated holder [18] throughout the acquisitions. The parameters described in the following were tested at constant flows provided by the phantom, as reported in Table 2.

Table 2. Flow rate settings for each test parameter.

Test parameter	Flow mode	Flow rate (ml·s^{-1})
AMVS	constant	5.5 and 7.0
VeMeA	constant	7.0
VPDI	constant	7.0
LDS	constant	2.0

B. Test parameters

The average maximum velocity sensitivity is a sensitivity parameter developed to quantify the US diagnostic system response to flow variations provided by a reference test device [14]. The objective measurement method, proposed and investigated in [14], post-processes PWD spectrograms acquired at two different constant flow rates (Q_1 and Q_2) and allows AMVS calculation as:

$$AMVS = \frac{v_{PW,Q2} - v_{PW,Q1}}{v_{th,Q2} - v_{th,Q1}} \quad (1)$$

where $v_{PW,Q1}$ and $v_{PW,Q2}$ are the mean maximum velocity values retrieved at Q_1 and Q_2, respectively, while $v_{th,Q1}$ and $v_{th,Q2}$ are the corresponding theoretical maximum flow velocities provided by the phantom. In addition, the method estimates the standard deviation of the parameter through the uncertainty propagation law [14].

The velocity measurements accuracy parameter allows the assessment of US system accuracy in the estimation of mean scatterer velocity, as already proposed in [3] for Color Doppler QA. The implemented measurement method assesses the average velocity trend through time as the weighted average of each spectral line [19]. The processing is repeated for three correction angle settings (i.e., insonation angle ± 1°) and the overall mean velocity $\bar{v}_{PW}$ is computed. Finally, the parameter is estimated as follows:

$$VeMeA = \frac{\left|\bar{v}_{PW} - \bar{v}_{th}\right|}{\bar{v}_{th}} \quad (2)$$

where $\bar{v}_{th}$ is the corresponding theoretical mean flow velocity provided by the Doppler phantom. The standard deviation of the parameter is estimated by applying the uncertainty propagation law.

The velocity profile discrepancy index provides an estimation of faults in sample volume length and range gate registration accuracy [15,16], by quantifying the discrepancy between the actual velocities and the theoretical parabolic profile (under laminar flow assumption). As in [15,16], the sample volume (SV) was placed at six depths (from 35 to 37 mm and from 39 to 41 mm with steps of 1 mm) corresponding to six different positions with respect to the radius of the phantom tube. The objective measurement method estimates the mean maximum velocity v_{PW} for each pre-set SV depth, and calculates VPDI [15,16] as in the following:

$$VPDI = \sum_{i=1}^{N} \frac{\left(v_{PW,i} - v_{par,i}\right)^2}{\sigma_{tot,i}^2} \quad (3)$$

where N is the number of collected PWD spectrograms, v_{par} is the velocity value retrieved from the theoretical parabolic profile for a specific position with respect to the tube radius, and σ_{tot} is the total standard deviation estimated by considering the following uncertainty contributions [15,16]: the intrinsic flow dispersion of the maximum velocities, the electronic noise superimposed on the spectrogram and the uncertainty in the sample volume positioning with respect to the radius.

Finally, the Lowest Detectable Signal (LDS) parameter [17], allows quantifying the flow detectability (expressed in dB) in terms of maximum depth of penetration through the following mathematical expression:

$$LDS = \frac{1}{N}\sum_{k=1}^{N}\left(2 f_0 \alpha z_{SV,k} + G_{max,k} - G_{min,k}\right) \quad (4)$$

where f_0 (MHz) is the operating Doppler frequency, α (dB·cm^{-1}·MHz^{-1}) is the (mean) TMM attenuation coefficient, z_{SV} (cm) is the sample volume depth setting, G_{max} (dB) is the maximum Doppler gain value before no negligible noise appears, while G_{min} (dB) is the minimum Doppler gain value at which the Doppler signal can no longer be distinguishable from background noise. The measurement method for G_{min} and G_{max} automatic assessment, investigated in [17], requires data to be collected by varying the Doppler gain from the minimum to the maximum with steps of ΔG for each sample volume depth setting. In this case, steps of 5 dB were applied and repeated for six SV depths (38 to 48 mm) spaced of 2 mm, by adjusting the sample volume in the center of the tube diameter. Specifications of each objective measurement method included in this study are listed in Table 3.

Since the optimal value differs per test parameter, a

Table 3. Variables setting for test parameters assessment.

AMVS [14]	Setting
Adaptive gray level threshold	10% of g_{max}
Number of spectral lines	800
VeMeA	
Number of spectral lines	800
VPDI [15,16]	
Adaptive gray level threshold	10% of g_{max}
Number of spectral lines	800
Minimum SV length increment	1 mm
Profile maximum velocity	v_{PW} at SVD_C
LDS [17]	
Threshold for G_{max} estimation	3
Threshold for G_{min} estimation	2
Regions of interest size	810×144 px
Cells size	6×6 px
Percentage of total cells	1%

g_{max}: maximum gray level value in the spectrogram; SVD_C: sample volume placed in the center of the phantom segment diameter.

parameter-specific mapping equation was applied to express each parameter in the range [0;1] where 1 represents the gold standard, as proposed in [3]. The following equations are used to express the scaled values, denoted with the symbol (*):

$$AMVS^* = 1 - \left(\left|AMVS - 1\right|\right) \tag{5}$$

$$VeMeA^* = \frac{1}{1 + VeMeA} \tag{6}$$

$$VPDI^* = e^{-VPDI/2.2} \tag{7}$$

$$LDS^* = \frac{LDS}{2\alpha f_0 z_{max}} \tag{8}$$

where z_{max} in (8) is the maximum phantom vessel depth. From the scaled values thus obtained, the Kiviat diagram areas were also calculated.

III. MONTE CARLO SIMULATION

The measurement uncertainty associated with the image analysis methods was estimated through a Monte Carlo Simulation (MCS) [20,21] run for 10^4 iterations for each test parameter-Doppler frequency pair. The standard deviations (SDs) of the output distributions retrieved for AMVS and VeMeA were then combined with the corresponding repeatability standard deviations.

Input distributions, expressed as mean ± SD, were assigned to the main quantities influencing each parameter assessment. For both AMVS and VPDI, a uniform distribution (10% ± 1% of the maximum gray level value in the spectrogram g_{max}) was assigned to the threshold for maximum velocities detection and the 800 spectral lines to be processed were randomized, at each cycle without repetition, among all the spectral lines in the image. As regards VeMeA parameter, the spectral lines randomization was applied only. Finally, for LDS assessment, a simulation was carried out for each *k*-th sample volume depth setting [17]: a normal distribution (0.700 ± 0.025 dB·cm^{-1}·MHz^{-1}) was assigned to TMM attenuation, while uniform distributions were chosen for the depth ($z_{SV,k}$ ± 0.3 cm) as well as to the minimum and maximum Doppler gain ($G_{min,k}$ ± 1 dB and $G_{max,k}$ ± 1 dB). The standard deviations of the *N* output distributions were then combined together to estimate the standard uncertainty contribution associated with the parameter.

IV. RESULTS AND DISCUSSION

Results on unscaled and scaled parameters for each test parameter at both operating Doppler frequencies are reported in Table 4. By comparing the outcomes obtained for the same test parameter, compatibility was always guaranteed according to the criterion in [22], however, a

Table 4. Outcomes and scaled outcomes (mean ± SD) for each test parameter according to the Doppler frequency.

Doppler frequency	Test parameter	Outcome	Scaled outcome	Normalized diagram area
Lowest operating frequency f_1	AMVS	0.93 ± 0.27	0.93 ± 0.27	0.45 ± 0.07
	VeMeA	0.96 ± 0.09	0.51 ± 0.02	
	VPDI	0.16 ± 0.07	0.93 ± 0.03	
	LDS	50.1 ± 2.3 dB	0.45 ± 0.02	
Central operating frequency f_2	AMVS	0.94 ± 0.28	0.94 ± 0.28	0.40 ± 0.06
	VeMeA	0.99 ± 0.09	0.50 ± 0.02	
	VPDI	0.25 ± 0.10	0.89 ± 0.04	
	LDS	53.7 ± 2.5 dB	0.38 ± 0.02	

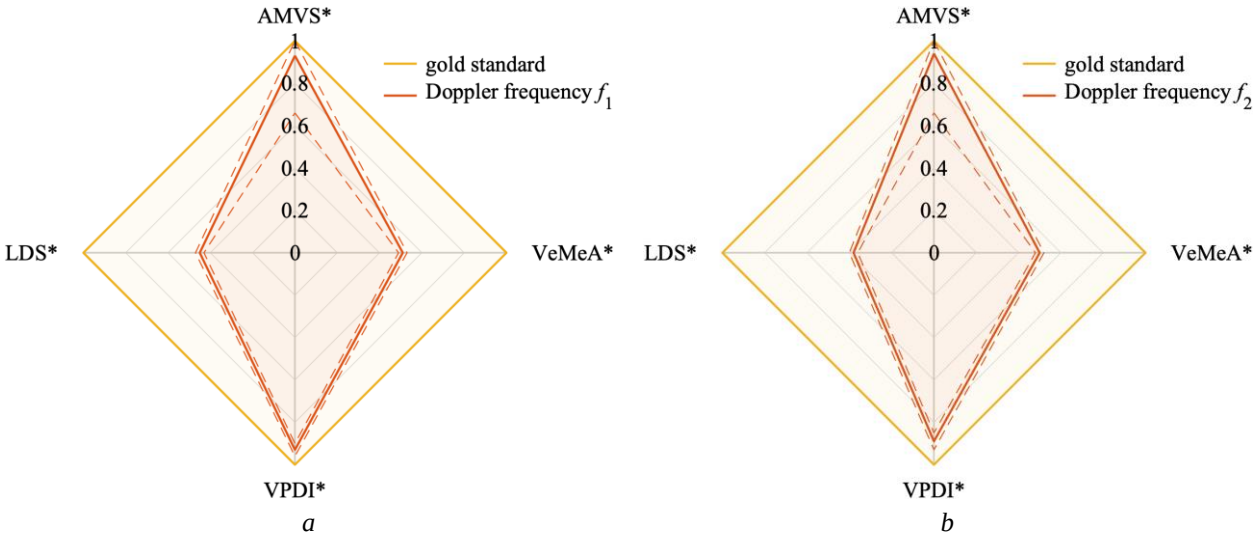

Fig. 1. Scaled outcomes represented on Kiviat diagram for the operating Doppler frequency (a) f_1 and (b) f_2.

proper comparison can be carried out by focusing on the scaled outcomes (Fig. 1). Independently of the operating frequency, the test parameters that significantly deviate from the gold standard were VeMeA and LDS, whilst AMVS parameter showed the highest uncertainty contribution. It is worth noting that, despite a higher LDS (absolute) value was retrieved at frequency f_2 rather than f_1, a better result (i.e., closer to 1) was obtained at the lower Doppler frequency after scaling. This behaviour, which was expected given the higher attenuation that affects high-frequency US waves, was outlined by the adopted scaling. As regards the Kiviat diagram areas, they were normalized with respect to the total area of the polygon (i.e., assuming all test parameters at 1), as in [3]. Therefore, the normalized diagram areas were expected to be as close as possible to 1. As reported in Table 4, they did not show discrepancies [22], suggesting compatible PWD performance between the two operating frequencies of the ultrasound probe.

V. CONCLUSIONS

The study herein proposed would give a contribution in the field of Doppler equipment QA by applying an integrated approach, already investigated in the literature, to PWD. This approach, based on the Kiviat diagram, allows summarizing the contribution of different QA parameters to quantify the overall performance of the US system. In this first study, four test parameters were objectively assessed through the post-processing of PWD spectrograms collected on a commercial reference test device. A linear array probe mounted on an intermediate technology level US diagnostic system was tested at two operating Doppler frequencies. The results obtained suggest that further investigations should be carried out on different phantom and US system settings, as well as on a larger sample of ultrasound diagnostic systems and probes.

ACKNOWLEDGMENT

The Authors wish to thank Jan Galo of the Clinical Engineering Service at I.R.C.C.S. Children Hospital Bambino Gesù for administrative and technical support, and GE Healthcare for hardware supply and technical assistance in data collection.

REFERENCES

[1] J. E. Browne, “A review of Doppler ultrasound quality assurance protocols and test devices”, Phys. Med., vol.30, No.7, November 2014, pp.742-751.

[2] S. Russell, “Ultrasound quality assurance and equipment governance”, Ultrasound, vol.22, No.1, February 2014, pp.66-69.

[3] G. Fiori, A. Pica, S. A. Sciuto, F. Marinozzi, F. Bini, A. Scorza, “A comparative study on a novel quality assessment protocol based on image analysis methods for Color Doppler ultrasound diagnostic systems”, Sensors, vol.22, No.24, December 2022.

[4] J. Vachutka, L. Dolezal, C. Kollmann, J. Klein, “The effect of dead elements on the accuracy of Doppler ultrasound measurements”, Ultrasonic Imaging, vol.36, No.1, January 2014, pp.18-34.

[5] B. Weigang, G. W. Moore, J. Gessert, W. H. Phillips, M. Schafer, “The methods and effects of transducer degradation on image quality and the clinical efficacy of diagnostic sonography”, J. Diagn. Med. Sonog., vol.19, No.1, January/February 2003, pp.3-13.

[6] M. Mårtensson, M. Olsson, L.-Å. Brodin, “Ultrasound transducer function: annual testing is not sufficient”, Eur. J. Echocardiogr., vol.11, No.9, October 2010, pp.801-805.

[7] M. Mårtensson, M. Olsson, B. Segall, A. G. Fraser, R. Winter, L.-A. Brodin, “High incidence of defective ultrasound transducers in use in routine clinical

practice", Eur. J. Echocardiogr., vol.10, No.3, May 2009, pp.389-394.

[8] N. J. Hangiandreou, S. F. Stekel, D. J. Tradup, K. R. Gorny, D. M. King, "Four-year experience with a clinical ultrasound quality control program", Ultrasound Med. Biol., vol.37, No.8, August 2011, pp.1350-1357.

[9] AIUM Technical Standards Committee, "Performance criteria and measurements for Doppler ultrasound devices", 2nd edition, USA, 2002.

[10] IPEM – Institute of Physics and Engineering in Medicine, "Report no. 102: Quality assurance of ultrasound imaging systems," York, UK, 2010.

[11] ACR Guidelines and Standards Committee, "ACR–AAPM Technical standard for diagnostic medical physics performance monitoring of real time ultrasound equipment", revised 2021, https://www.acr.org/-/media/ACR/Files/Practice-Parameters/US-Equip.pdf (accessed June 2023).

[12] EFSUMB, "European course book: technical quality evaluation of diagnostic ultrasound systems - a comprehensive overview of regulations and developments", http://www.kosmos-host.co.uk/efsumb-ecb/coursebook-tqe_ch28.pdf (accessed June 2023).

[13] J. M. Samei, D. E. Pfeiffer, "Clinical Imaging Physics: Current and Emerging Practice", 1st edition, Wiley Blackwell, Hoboken, NJ, USA, 2020.

[14] G. Fiori, F. Fuiano, A. Scorza, M. Schmid, J. Galo, S. Conforto, S. A. Sciuto, "A novel sensitivity index from the flow velocity variation in quality control for PW Doppler: a preliminary study," Proc. of 2021 IEEE International Symposium on Medical Measurements and Applications (MeMeA), 2021.

[15] G. Fiori, G. Bocchetta, S. Conforto, S. A. Sciuto, A. Scorza, "Sample volume length and registration accuracy assessment in quality controls of PW Doppler diagnostic systems: a comparative study", ACTA IMEKO, vol.12, No.2, June 2023, pp.1-7.

[16] G. Fiori, A. Scorza, M. Schmid, J. Galo, S. Conforto, S. A. Sciuto, "A preliminary study on a novel approach to the assessment of the sample volume length and registration accuracy in PW Doppler quality control," Proc. of 2022 IEEE International Symposium MeMeA on Medical Measurements and Applications (MeMeA), 2022.

[17] G. Fiori, F. Fuiano, A. Scorza, J. Galo, S. Conforto, S. A. Sciuto, "A preliminary study on an image analysis based method for lowest detectable signal measurements in pulsed wave Doppler ultrasounds", ACTA IMEKO, vol.10, No.2, June 2021, pp.126-132.

[18] Sun Nuclear Corporation, "Doppler 403™ & mini-Doppler 1430™ flow phantoms", https://www.sunnuclear.com/uploads/documents/datasheets/Diagnostic/DopplerFlow_Phantoms_113020.pdf (accessed June 2023).

[19] F. Marinozzi, F. Bini, A. D'Orazio, A. Scorza, "Performance tests of sonographic instruments for the measure of flow speed," Proc. of 2008 IEEE International Workshop on Imaging Systems and Techniques (IST), 2008.

[20] JCGM 101:2008, "Evaluation of measurement data — Supplement 1 to the Guide to the expression of uncertainty in measurement — Propagation of distributions using a Monte Carlo method", 2008, https://www.bipm.org/documents/20126/2071204/JCGM_101_2008_E.pdf/325dcaad-c15a-407c-1105-8b7f322d651c (accessed June 2023).

[21] G. Bocchetta, G. Fiori, A. Scorza, S. A. Sciuto, "Image quality comparison of two different experimental setups for MEMS actuators functional evaluation: a preliminary study," Proc. of the 25th IMEKO TC4 International Symposium & 23rd International Workshop on ADC and DAC Modelling and Testing, 2022.

[22] J. R. Taylor, "An Introduction to Error Analysis: the Study of Uncertainties in Physical Measurements", 2nd edition, Univ. Science Books, Sausalito, USA, 1996.